Збірник наукових праць. Галузеве машинобудування, будівництво
Academic journal. Industrial Machine Building, Civil Engineering
http://journals.nupp.edu.ua/znp
https://doi.org/10.26906/znp.2025.65.4215

UDC 624.012

Petro Reznik *
O.M. Beketov National University of Urban Economy in Kharkiv
https://orcid.org/0000-0003-3937-6833

Anton Volodymyrov
O.M. Beketov National University of Urban Economy in Kharkiv
https://orcid.org/0009-0001-8416-535X

Dzhamaldii Alataiev
O.M. Beketov National University of Urban Economy in Kharkiv
https://orcid.org/0000-0003-1570-8469

Vladyslav Maksymenko
O.M. Beketov National University of Urban Economy in Kharkiv
https://orcid.org/0009-0007-3771-0857

Experimental and numerical study of full-scale reinforced concrete beams with 3DCP permanent formwork

Abstract. The performance of a box-type permanent 3DCP formwork for full-scale reinforced concrete beams was assessed through experimental testing and numerical analysis. Eight beams were tested under four-point bending to examine the contribution of the printed shell to stiffness, crack development, and load-bearing capacity. The specimens exhibited a flexural–shear failure mechanism, while no delamination between the printed shell and the cast-in-place core was observed. A nonlinear finite element model was calibrated against the experimental load–deflection responses and then used for comparative simulations. The predicted ultimate load was 81.9 kN for beams with 3DCP formwork and 77.1 kN for a numerically simulated reference beam without formwork. An energy-based assessment showed that the total strain energy decreased to 49.64 % at the same load level, indicating increased stiffness and improved efficiency of the composite cross-section.

Keywords: 3D concrete printing (3DCP), permanent formwork, reinforced concrete beam, finite element method, strain energy

*Corresponding author E-mail: Petro.Reznik@kname.edu.ua

Received: 02.12.2025 Accepted: 18.12.2025 Published: 26.12.2025

Introduction.

Additive technologies in construction, particularly 3D printing with cementitious composites, are gradually evolving from demonstration projects toward engineering-based solutions for load-bearing elements. In the “roadmap” proposed by Buswell [1], the key scientific and technological challenges of extrusion-based 3D concrete printing are identified: control of rheology and buildability, ensuring repeatability of material properties, managing interlayer bonding, and integrating the technology with structural analysis and standardization. The review by Jipa and Dillenburger [2] highlights that one of the most practical implementation paths is the use of 3D printing for producing formwork of complex geometry, followed by conventional concreting and reinforcement. At the same time, a synthesis of reinforcement methods for 3D-printed concrete confirms that reinforcement integration, interface reliability, and construction tolerances remain decisive factors for scaling up to real structures [3].

One promising direction is 3D-printed permanent formwork which, after concreting, not only shapes the cross-section but can also contribute structurally to load transfer. The feasibility of this concept has been experimentally demonstrated for columns, where force transmission through the “shell–core” contact interface is critical [4]. For slabs and slab systems, digital form-generation enables the realization of efficient thin-walled shells, including topology-optimized and mineral-printed forms [5,6]. Composite slabs with an active structural role of the printed formwork have been developed, including prestressed systems [7], as well as a series of studies on ribbed slabs where load transfer, flexural performance, and the influence of rib and void geometry on strength and cracking resistance were

examined [8–10]. Alternative material solutions for permanent formwork, such as textile-reinforced concrete for composite slabs [11], further emphasize the overall trend: the shell is increasingly treated as a structural component rather than merely as form. For thin-walled elements, serviceability aspects such as fire resistance of high-strength printed panels also become relevant [12]. A major limitation remains the layered nature of 3D-printed materials and the resulting anisotropy of properties, which directly affects shell cracking and interface behavior [3,13].

The most relevant studies for transition toward frame systems concern reinforced concrete beams with 3D-printed permanent formwork. Full-scale experiments confirm that the shell can enhance stiffness, crack resistance, and energy absorption at failure; however, the outcome strongly depends on structural detailing and compatibility conditions between materials [14]. It has also been shown that for such elements, the interaction between bending and shear behavior and the control of local damage zones is critical [15]. The concept of off-site fabrication followed by concreting is of practical importance for improving repeatability and process control [16], as is the comparison of reinforcement strategies and their effect on failure mechanisms [17]. Additional technological approaches address the integration of longitudinal reinforcement during printing [18] and the coordination of printing and reinforcement trajectories for manufacturing reinforced elements [19]. For the hybrid scheme "3D-printed permanent formwork + conventional concrete core," both structural efficiency and technological feasibility have been experimentally validated [20]. Improvements in crack resistance and deformability may also be achieved through the shell material itself, including deformable geopolymer-based composites [21] and high-strength shells with controlled (including graded) fiber reinforcement [22]. For shear performance and interface behavior, important findings have been obtained for beams with textile permanent formwork [23], numerical studies of shear response of beams with 3D-printed formwork [24], and solutions where the printed shell functions as transverse reinforcement or shear control [25,26]. In the Ukrainian context, recent studies confirm the applicability of 3D printing for spatial structural models [27] and explore printed formwork for monolithic beams with integrated reinforcement channels [28], which is essential for the development of a local technological base.

Despite significant progress at the level of individual elements, there remains a lack of research directly focused on the development of integrated frame systems with repeatable joints and reliable load transfer between components. In this regard, structural continuity – particularly the uninterrupted passage of longitudinal reinforcement through "column–beam" joints – is essential for composite frame action. For such systems, it is necessary to combine experimental results with validated numerical models of the composite cross-section and interface, as previously substantiated in numerical investigations of 3D-printed permanent formwork for reinforced concrete [29], taking into account the established anisotropy of 3D-printed concrete [13]. To compare alternatives and generalize results, an energy-based approach employing the distribution of deformation potential energy as an integral assessment criterion is recommended [30,31]. Its relevance for optimization problems has been demonstrated for topology-optimized reinforced concrete slabs [32] and for improving the parameters of hybrid "shell–core" structural systems [33]. The significance of permanent formwork as an active structural layer is confirmed not only for 3D-printed systems: recent studies have shown that prefabricated UHPC permanent formwork panels with embedded steel meshes and specially configured contact surfaces (ribs, shear keys) can substantially enhance the flexural behavior of reinforced concrete beams – doubling the cracking load, increasing stiffness, and improving ultimate load capacity by approximately 30%, with the effect largely governed by interface bond quality and detailing [34].

Therefore, the experimental investigation of full-scale reinforced concrete beams with 3D-printed box-type permanent formwork is considered a necessary step toward substantiating a frame-based structural solution in which interface phenomena, shell anisotropy, reinforcement detailing, and energy-based performance criteria are integrated within a unified methodology suitable for further numerical validation and for application to repeatable structural joints and elements.

Problem statement.

The aim of this research is the experimental investigation of the influence of box-type permanent formwork manufactured by 3DCP technology on the stiffness, crack resistance, and ultimate load-bearing capacity of full-scale reinforced concrete beams subjected to four-point bending.

Object of the study is full-scale reinforced concrete beams with box-type 3D-printed permanent concrete formwork.

Subject of the study – the stress-strain state of full-scale reinforced concrete beams under four-point bending and its evolution during the stages of cracking and failure, including deflections, concrete and reinforcement strains, and the fields of normal and shear stresses in critical regions. Additionally, the study examines the influence of the 3D-printed permanent formwork, transverse reinforcement, and local technological defects on the distribution of these SSS components, as well as on stiffness, crack resistance, and ultimate load capacity.

Research objectives can be defined as follows:

- To perform experimental testing of a series of full-scale beams with 3D-printed permanent formwork under a four-point bending scheme and to obtain load–deflection curves, as well as cracking and strain data from strain gauges.
- To compare the performance of beams with and without transverse reinforcement and to assess the effect of a local formwork defect.

- To compare the experimental results with the code-based load-bearing capacity evaluation according to DSTU B V.2.6-156:2010 [35].
- To conduct numerical verification in ANSYS and to compare calculated and experimental stress–strain and load capacity parameters.
- To perform an energy-based interpretation of beam behavior in LIRA 10.16 using the strain energy criterion for cases with and without the printed formwork.

Main material and results.

The investigated structural element is a composite shell–core system in which the 3D-printed concrete shell serves as permanent formwork and simultaneously participates in the structural behavior of the cross-section, while the core is formed by casting conventional concrete inside the shell. The overall beam geometry is as follows: length L = 3220 mm, width b = 200 mm, and height h = 320 mm. The thickness of the 3DCP formwork is 60 mm at the bottom and 40 mm at each side wall; the core dimensions are 120 mm in width and 260 mm in height. General view for experimental specimens is shown in Fig. 1.

Figure 1 – General view of a test specimen

Compressive strength was direction-dependent due to the layered 3DCP fabric. The highest value, 17.3 MPa, was obtained under loading perpendicular to the printed layers (vertical compression), whereas 12.3-12.4 MPa was measured under loading parallel to the layers, both along and across the extrusion paths; the material performance corresponds approximately to concrete class C16/20. The beam core was produced from conventional concrete of class C20/25.

The experimental program included eight full-scale beams of identical geometry and longitudinal reinforcement layout. To ensure reliable comparison of structural parameters, all specimens were fabricated using a unified fabrication/technological procedure with consistent conditions for shell printing, reinforcement placement, and core casting. The primary controlled variables were the presence of transverse reinforcement and the integrity of the 3DCP shell prior to testing.

Longitudinal reinforcement for all beams consisted of 4Ø10 A500C bars in the tensile zone and 2Ø10 A500C bars in the compression zone.

Based on the presence of transverse reinforcement and the condition of the shell, the beams were divided into three groups.

The first group (specimens B1–B5, Fig. 1, a) comprised beams with transverse reinforcement in the form of Ø6 A500C stirrups spaced at 200 mm, with no observed local shell damage.

The second group (specimens B6–B7, Fig. 1, b) included beams without transverse reinforcement, containing only minimum (nominal) reinforcement formed by several Ø6 A500C bars; no local shell defects were detected.

The third group (specimen B8) was a beam with Ø6 A500C stirrups at 200 mm spacing and with local defects of the 3DCP shell that existed before testing. These defects appeared as localized shell damage/failure in the midspan region and in the near-support zones.

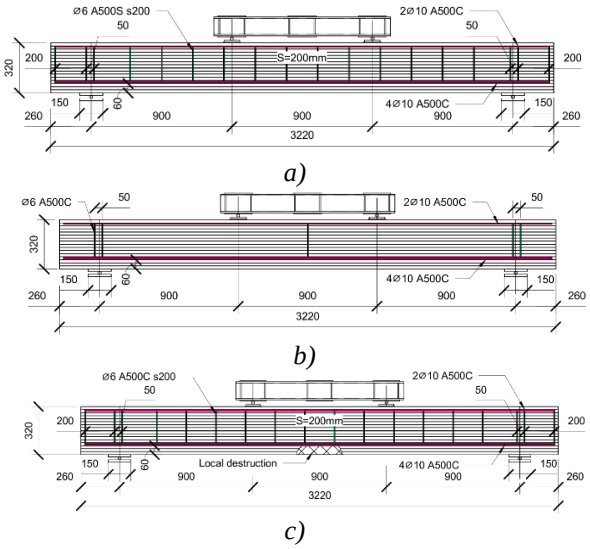

Figure 2 – Test series: a) – with transverse reinforcement, b) – without transverse reinforcement, c) – transverse reinforcement and local destruction

Beam tests were carried out using a four-point bending scheme (see Fig. 3), creating a constant-moment region between the load application points. The beam was supported on two hinged supports (a pinned support and a roller support), while the load was applied through a distribution beam that ensured force transfer to two loading points.

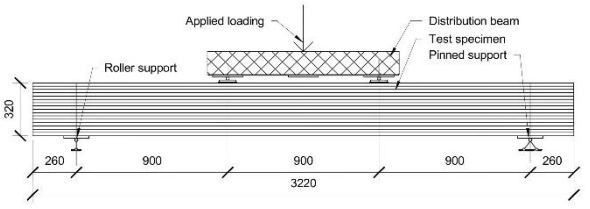

Figure 3 – Loading scheme with a distribution beam

The load was generated by a hydraulic jack with a capacity of 500 kN, installed in a reaction portal frame anchored to the strong floor using anchor elements. The

structural configuration of the loading frame is shown in Fig. 4.

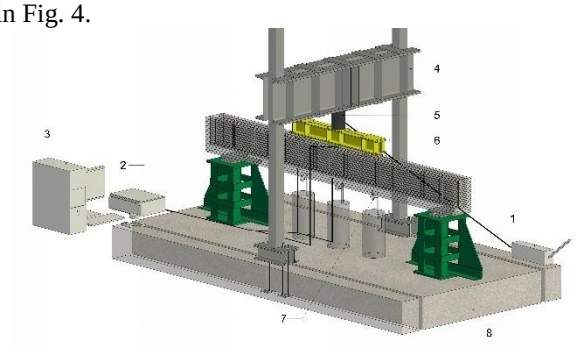

Figure 4 – Testing reaction portal frame

Vertical displacements of the beam were measured using dial gauges with a resolution of 0.01 mm. The gauges were installed at three characteristic locations: at midspan and beneath the two load application points, allowing both global deflection and local displacements in the loading zones to be monitored. Strain gauges were placed in the region of maximum bending moment (midspan), specifically on the top surface to record compressive strains and on the bottom surface to record tensile strains. This arrangement provided direct monitoring of the evolution of the stress–strain state during loading.

During the experiment, visual crack monitoring was performed on the outer surface of the 3DCP shell; therefore, the observed crack pattern reflects the behavior of the shell as part of the composite shell–core system. Crack height development was evaluated based on the number of 3D printing extrusion layers, where one extrusion corresponds to one layer with a thickness of approximately 20 mm. Crack width was not measured instrumentally because the layered surface relief and local anisotropy of the 3DCP shell make reliable microscope-based readings impractical and non-repeatable under the given test conditions. Therefore, crack development was assessed by visual monitoring and by crack height quantified in terms of the number of crossed printed layers.

Experimental tests.

For all specimen series, a flexural–shear failure mechanism was observed, characterized by the formation of a dominant inclined crack in the near-support region. This crack propagated from the load application zone toward the support and governed the ultimate limit state.

Photographic documentation of cracking demonstrated that the 3D-printed permanent shell acted as an integral part of the composite shell–core cross-section rather than as an unanchored cladding. During loading and after reaching the ultimate state, no extensive delamination of the shell from the concrete core was observed, indicating effective transfer of shear forces across the interface and compatibility of deformations between the components. Since cracks were recorded on the external surface of the shell, the resulting crack pattern represents the stress–strain state of the shell within the composite element and can be directly correlated with strain gauge data and measured deflections. The characteristic stages of structural behavior are shown in Fig. 5 and can be described as follows: 1. pre-cracking stage (<24 kN); 2. onset of flexural cracking (24–40 kN); 3. transition to flexural–shear behavior (inclined cracks with a development height of approximately 3–11 extrusion layers); 4. ultimate limit state and failure.

Figure 5 – Characteristic stages of structural behavior of test specimen

The experimental ultimate values of internal forces in most specimens exceed the code-based flexural capacity estimated using the deformation-based procedures of DSTU [35]. The calculated flexural capacity for the beam with 3DCP formwork is M = 34.2 kNm, whereas for the conventional beam it is M = 32.7 kNm. The graph in Fig. 6 shows that all specimens, except B6, exhibit ultimate moments that are above or close to 34.2 kNm, while the value for B6 is at the level of the calculated moment for the conventional cross-section. Overall, this confirms that the actual flexural load-bearing capacity of the tested elements is not lower than the code-predicted value, and that the DSTU-based calculation provides a conservative baseline estimate.

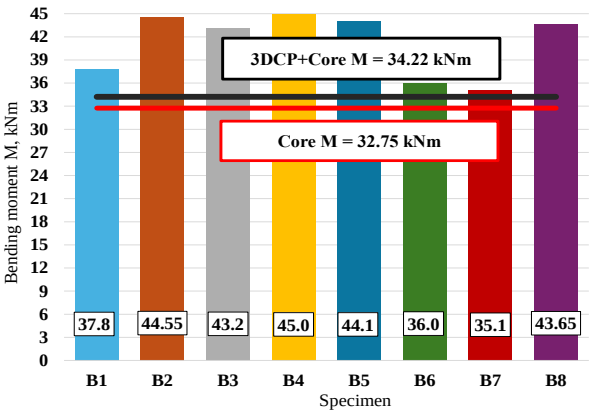

Figure 6 – Comparison of ultimate bending moments M_u for specimens B1–B8 determined from experimental results with the code-based value according to [35]

The comparison in terms of shear force shows a clearer differentiation between the specimen series. For

specimens with transverse reinforcement, the code-based evaluation yields V = 49.1 kN for the system with 3DCP formwork and V = 39.7 kN for the conventional beam. For the series without transverse reinforcement, the calculated values are lower: V = 34.6 kN for the 3DCP system and V = 22.5 kN for the conventional cross-section. The experimental shear force values for specimens B1–B5 are close to or exceed 49 kN, which is consistent with the contribution of transverse reinforcement at the final stage and the development of a flexural–shear failure mechanism. For specimens without transverse reinforcement, B6–B7, a reduction of the ultimate shear force to approximately 39-40 kN was recorded; however, these values still significantly exceed the code-based estimate for a conventional cross-section without stirrups, confirming the contribution of composite shell–core action to shear resistance.

The defective specimen B8 exhibits high ultimate values for both bending moment M and shear force V, comparable to the best results within the series. This is consistent with the fact that local shell damage affects the local crack pattern but does not necessarily reduce the ultimate internal forces, provided that shear transfer across the interface is not disrupted and the overall structural integrity of the element is maintained up to the failure stage.

For each specimen, load-strain relationships ε in the compressed zone were constructed (see Fig.7). The curves exhibit a monotonic character with a more pronounced increase in strains at the final stages, corresponding to stiffness degradation after cracking and redistribution of internal forces within the cross-section. The obtained relationships are used as instrumental confirmation of the behavior of the compressed zone and for comparison with deformability derived from load–displacement diagrams, as well as for verification of numerical models.

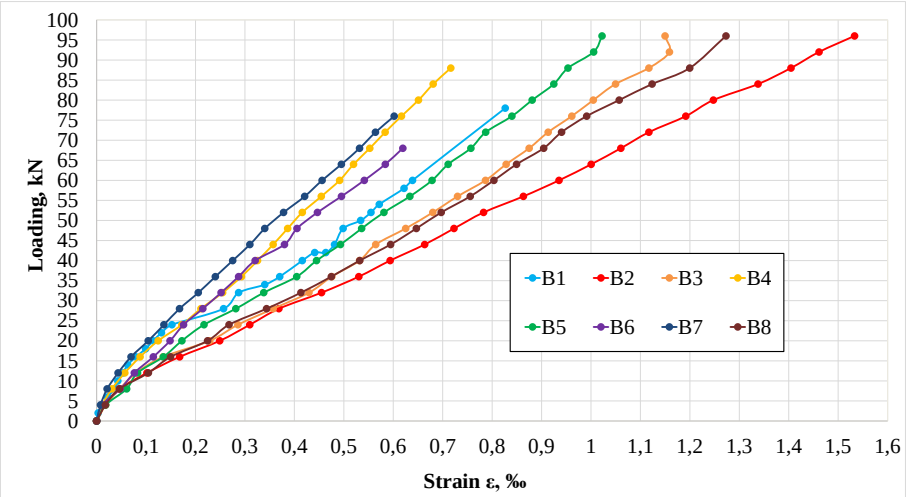

Figure 7 – Load–strain ε relation in the concrete core in the compressed zone near the top fiber based on strain gauge measurements

Numerical analysis.

Since the experimental tests were performed on beams with permanent 3D-printed formwork, numerical verification at the first stage was carried out for the same structural configuration, reproducing the geometry, boundary conditions, and loading scheme. After achieving agreement between the numerical results and the experimental data within the adopted assumptions, a second stage of analysis was performed in which analogous beams without permanent formwork were modeled, enabling a consistent comparison of the influence of the formwork on the integral performance parameters of the element.

Numerical verification was conducted in ANSYS Workbench (Static Structural) using a nonlinear formulation with consideration of large displacements (see FE model in Fig. 8). The geometry was created in Autodesk Revit, exported in SAT format, and imported into ANSYS SpaceClaim; simplification was performed by removing local irregularities associated with the layered 3D printing process, and smooth contact surfaces were prepared to allow proper finite element meshing and accurate contact interaction modeling.

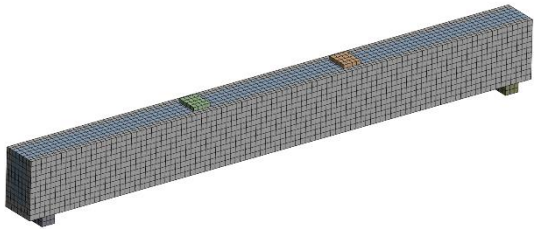

Figure 8 – Finite element model in ANSYS

Both the 3DCP shell and the cast-in-place core were modeled as a shell–core system and assigned concrete classes C16/20 and C20/25, respectively (E = 29 GPa and 30 GPa, ν = 0.20). Concrete nonlinearity was represented using a Microplane constitutive model implemented via APDL for a 3D microplane solid, with strength parameters consistent with the selected concrete classes.

Longitudinal rebars Ø10 and stirrups Ø6 were included by their cross-sectional areas; steel was modeled as linear elastic (E = 200 GPa, ν = 0.30) with a perfect-bond assumption (no slip).

Composite action between the shell and the core was enforced by an ideal tied connection using shared nodes along the interface. The load introduction region was defined as bonded contact, while the supports were reproduced using no-separation contact on one side and frictional contact on the other (μ = 0.7). The analysis was performed under displacement control up to 1.5 mm, and the reaction force was used to build the load–displacement curve; nonlinear equilibrium was solved using automatic substepping with the Newton–Raphson scheme.

The load–displacement curve (see Fig. 9) obtained in ANSYS for the specimen with permanent formwork falls within the experimental scatter and accurately reproduces the response envelope over the main loading range and the final failure stage. This agreement confirms the adequacy of the adopted boundary conditions, contact formulation, and stiffness parameters of the numerical model.

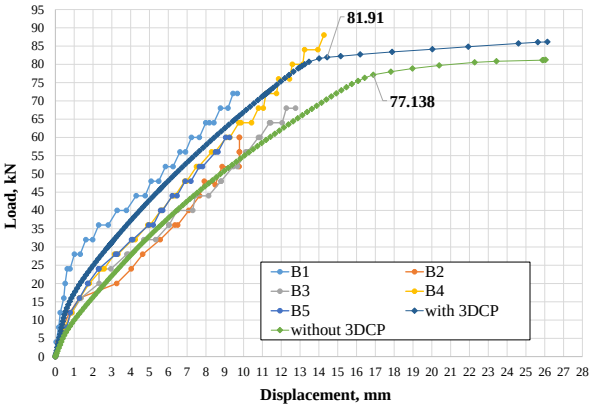

Figure 9 – Load–displacement curves for specimens B1–B5 and numerical simulation results obtained in ANSYS for beams with and without 3DCP permanent formwork

A similar level of correlation for 3DCP elements has been reported by other researchers using nonlinear concrete constitutive models and properly defined contact interfaces [24], [29]. The moderate increase in ultimate load observed in the stirrup-reinforced series is therefore expected. In studies involving permanent formwork, the contribution is often more pronounced in terms of stiffness and crack resistance, whereas the gain in peak load may remain limited, even for higher-strength UHPC panels [34].

The distribution and magnitude of deflections are consistent with the shape of the experimental load–displacement curves and explain the lower deformation energy capacity observed for the specimen with permanent formwork. In the configuration without formwork, larger maximum displacements are recorded at a lower ultimate load, which corresponds to the reduced flexural stiffness of the cross-section.

For the beam with 3DCP permanent formwork, the maximum displacements are smaller, while the corresponding load level is higher. This behavior is consistent with the expected increase in the second moment of area and the composite action between the shell and the core. A similar response has been reported in studies where a composite section with a permanent layer reduces deformability under the same external actions [34].

Deformations (see Fig. 10) localize in regions where cracking is expected, particularly within the pure bending zone and the shear spans. In the specimen without permanent formwork, strain localization occurs earlier and is more pronounced, which is consistent with the lower stiffness and the faster transition to the cracked stage.

In contrast, for the specimen with 3DCP permanent formwork, the strain field is more uniformly distributed at higher load levels. This behavior is attributed to a more efficient redistribution of deformations within the composite cross-section.

The maximum principal elastic strains ε recorded under loading were as follows (see Fig. 11): for the beam without 3D-printed concrete formwork, ε ranged from 1.60×10^{-4} to 3.97×10^{-6} at a load of 77.138 kN; for the beam with 3D-printed concrete permanent formwork, ε ranged from 1.72×10^{-4} to -1.33×10^{-7} at a load of 81.912 kN.

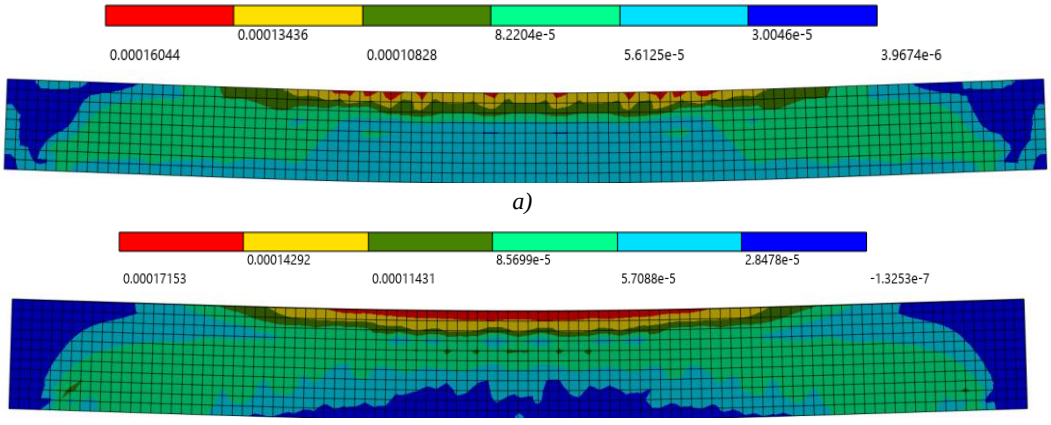

Figure 10 – Maximum principal elastic strains ε under loading in the beams: a) – without permanent formwork; b) – with permanent formwork

The maximum shear stresses develop within the shear spans and in the contact zones at the supports and load application points. This behavior is consistent with the formation of inclined cracks.

The shear stresses τ recorded under loading were as follows (see Fig. 11): for the beam without 3D-printed concrete formwork, τ ranged from 2.53 to −2.53 MPa at a load of 77.138 kN; for the beam with 3D-printed concrete permanent formwork, τ ranged from 1.94 to −1.96 MPa at a load of 81.912 kN.

For the specimen with permanent formwork, shear stresses of approximately τ = 1.94 to −1.96 MPa are reached at a higher load level, while the stress field remains symmetric. In the specimen without formwork, the shape of the shear stress field is similar, but the ultimate load is lower.

The difference between the two configurations can be attributed to the influence of the composite cross-section on shear stiffness and on the transfer of shear stresses at the shell–core interface. This mechanism has also been highlighted in studies that consider permanent formwork as an active structural layer [34].

The principal stress field reveals tensile and compressive zones that govern crack initiation. The maximum tensile stresses, on the order of 1 MPa, are physically consistent with the tensile strength of concrete for the adopted material classes.

In both models, the topology of the tensile zones is similar, confirming the adequacy of the applied loading and support scheme. For the specimen with permanent formwork, the region of elevated σ develops at a higher load level without signs of unstable asymmetry, which is consistent with the stiffer response and improved shear transfer in the composite cross-section.

The maximum principal stresses σ (see Fig. 12) recorded in the beams under loading were as follows: for the beam without 3D-printed concrete formwork, σ = 0.98 MPa at a load of 77.138 kN; for the beam with 3D-printed concrete permanent formwork, σ = 1.00 MPa at a load of 81.912 kN.

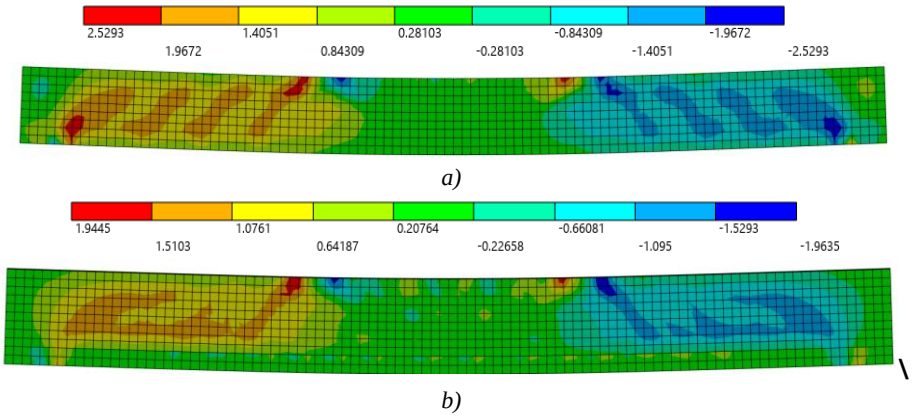

Figure 11 – Shear stresses (τ) in the beams under loading: (a) without permanent formwork; (b) with permanent formwork

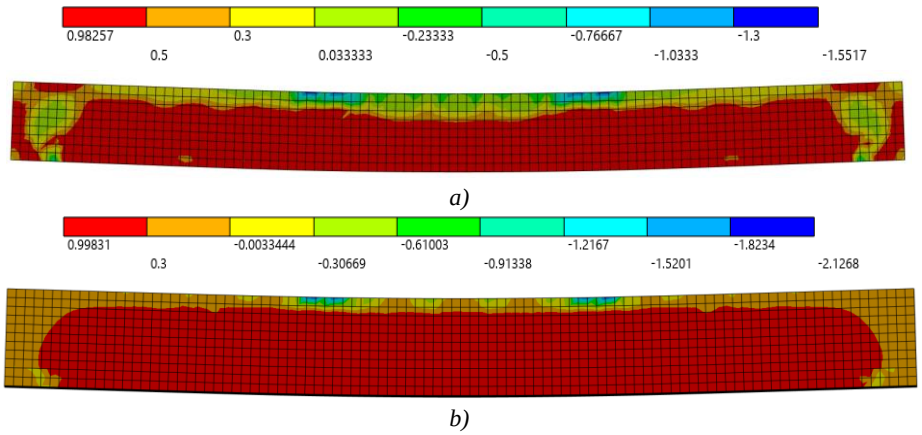

Figure 12 – Maximum principal stresses σ in the beams under loading: (a) without permanent formwork; (b) with permanent formwork

The numerical verification performed in ANSYS confirms good agreement with the experimental results in terms of the key response features, including the deflection shape, localization of compression in the upper zone, concentration of shear stresses in the shear spans, and the correspondence between critical regions and the strain fields. This is consistent with the approaches adopted in international studies on 3DCP elements and systems with permanent formwork [24], [29], [34].

The comparative results for the model without formwork are physically consistent and demonstrate

the expected reduction in stiffness and ultimate load. The advantage of the 3DCP permanent formwork in the present series is primarily manifested in the increased stiffness and the more favorable shear response of the composite cross-section, whereas the gain in peak load in the presence of transverse reinforcement remains moderate and follows the general trend reported for permanent formwork systems, including UHPC solutions [34].

To provide an integral assessment of the effect of 3DCP permanent formwork, additional analyses were performed in LIRA 10.16 using the Vasilkov–Shmukler energy criterion for beams with and without formwork. For both configurations, identical boundary conditions and loading schemes were adopted. The evaluation was based on the fields of strain energy density as well as on the total strain energy of the system.

The distributions of strain energy density (see Fig. 13) revealed its localization in the regions of normal crack formation within the pure bending zone and in the near-support regions where inclined cracks develop. Maximum values were also observed in the contact areas at the load application points and supports, which corresponds to stress concentration in these zones. The identified regions of increased strain energy density are consistent with the experimentally observed crack patterns and the flexural–shear failure mechanism recorded during testing. Therefore, strain energy density can be regarded as an informative integral damage indicator for the composite shell–core system.

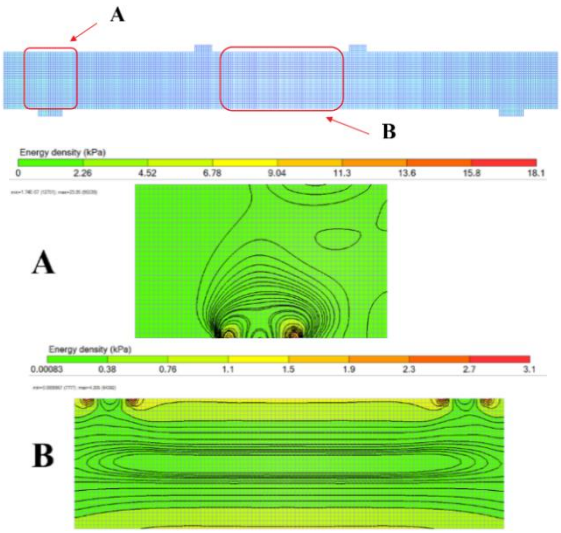

Figure 13 - Strain energy density field

A comparison of the total strain energy for the two configurations showed a substantial difference. For the RC+3DCP variant, the total strain energy was reduced to 49.64% of that of the RC beam under the same loading regime. The total strain energy was compared at the same external load level, while the resulting displacements and stress fields differed due to the stiffness contrast of the analyzed cross-sections. This result can be interpreted as an increase in structural stiffness associated with the use of 3DCP permanent formwork, which is attributed to the enhanced cross-sectional stiffness and the composite action between the shell and the core.

This behavior is also consistent with the improved ability of the composite system to transfer shear stresses, which govern the development of inclined cracks and the shear-dominated failure mechanism. Hence, provided that sufficient interaction is ensured at the shell–core interface, the use of 3DCP permanent formwork results in a stiffer structural response and a reduced deformation energy capacity, which is critical for assessing the reserve prior to the formation of a dominant inclined crack.

Conclusions.

The experimental testing of full-scale beams under a four-point bending scheme confirmed that all specimens failed according to a flexural–shear mechanism governed by the formation of a dominant inclined crack in the shear span. The first normal cracks were observed at loads of 24–40 kN, inclined cracks developed mainly within 76–100 kN, and failure occurred in the range of 92–128 kN. No continuous delamination between the 3D-printed permanent formwork and the concrete core was observed, which confirms their composite action up to the ultimate state. The comparison of specimens with and without transverse reinforcement demonstrated its governing role in stabilizing the shear response: the transition to the flexural–shear stage occurred earlier and more abruptly in beams without stirrups. The specimen with a local formwork defect exhibited only minor deviations in the initial cracking stage, while the overall failure mechanism remained unchanged. The code-based evaluation according to DSTU B V.2.6-156:2010 [35] predicted a small difference in flexural capacity (34.2 kNm vs. 32.7 kNm) but a much larger difference in shear capacity (34.6 kN vs. 22.5 kN), which was confirmed experimentally, indicating that shear governs the structural behavior of the tested series.

The numerical verification in ANSYS reproduced the key experimental features in terms of load–deflection response, stress–strain fields, and localization of critical zones. The calculated ultimate loads were 81.9 kN for the beam with 3DCP formwork and 77.1 kN for the reference beam, corresponding to a difference of about 6%. The beam with permanent formwork exhibited smaller deflections and higher stiffness, while the increase in peak load remained moderate due to the stabilizing effect of transverse reinforcement. The energy-based analysis performed in LIRA 10.16 using the strain energy criterion demonstrated a substantial reduction in total deformation energy for the RC+3DCP configuration, which reached only 49.64% of the value obtained for the conventional RC beam under the same loading scheme. These results confirm that the primary structural benefit of the 3D-printed permanent formwork lies in the enhancement of stiffness, improved shear transfer at the shell–core interface, and reduced deformation energy prior to the formation of the governing inclined crack.

The study is limited to one geometry and one shell thickness; therefore, the reported trends should be generalized with caution. Further work should address interface characterization (bond/shear transfer) and parametric variations of shell geometry and reinforcement.

References

1. Buswell, R. A., De Silva, W. L., Jones, S. Z., & Dirrenberger, J. (2018). 3D printing using concrete extrusion: A roadmap for research. *Cement and Concrete Research*, *112*, 37–49. https://doi.org/10.1016/j.cemconres.2018.05.006.
2. Jipa, A., & Dillenburger, B. (2022). 3D printed formwork for concrete: State-of-the-art, opportunities, challenges, and applications. *3D Printing and Additive Manufacturing*, *9*(2), 84–107. https://doi.org/10.1089/3dp.2021.0024.
3. Nan, B., Qiao, Y., Leng, J., & Bai, Y. (2025). Advancing structural reinforcement in 3D-printed concrete: Current methods, challenges, and innovations. *Materials*, *18*(2), 252. https://doi.org/10.3390/ma18020252.
4. Zhu, B., Nematollahi, B., Pan, J., et al. (2021). 3D concrete printing of permanent formwork for concrete column construction. *Cement and Concrete Composites*, *121*, 104039. https://doi.org/10.1016/j.cemconcomp.2021.104039.
5. Jipa, A., Bernhard, M., Meibodi, M., et al. (2016). 3D-printed stay-in-place formwork for topologically optimized concrete slabs. In *TxA Emerging Design + Technology* (pp. 97–107). UCL Press. https://doi.org/10.3929/ethz-b-000237082
6. Bedarf, P., Calvo-Barentin, C., Martinez Schulte, D., Şenol, A., Jeoffroy, E., & Dillenburger, B. (2023). Mineral composites: Stay-in-place formwork for concrete using foam 3D printing. *Architecture, Structures and Construction*, *3*(2), 251–262. https://doi.org/10.1007/s44150-023-00084-x.
7. Guan, J., Wang, L., Huang, Y., & Ma, G. (2025). 3D printed concrete composite slabs fabricated by prestress reinforced permanent formwork: Design, manufacturing, and performance. *Engineering Structures*, *325*, 119446. https://doi.org/10.1016/j.engstruct.2024.119446.
8. Raza, S., Manshadi, B., Sakha, M., Widmann, R., Wang, X., Fan, H., & Shahverdi, M. (2025). Load transfer behavior of 3D printed concrete formwork for ribbed slabs under eccentric axial loads. *Engineering Structures*, *322*, 119148. https://doi.org/10.1016/j.engstruct.2024.119148.
9. Raza, S., Sakha, M., Hassan, Z., Manshadi, B., Wang, X., Fan, H., Dillenburger, B., & Shahverdi, M. (2025). Flexural behavior of stay-in-place load-bearing 3D-printed concrete formwork for ribbed slabs. *Engineering Structures*, *338*, 120531. https://doi.org/10.1016/j.engstruct.2025.120531.
10. Sakha, M., Raza, S., Wang, X., Fan, H., Pichler, N., & Shahverdi, M. (2026). Design optimization and assessment of stay-in-place 3D printed concrete formwork for slabs. *Automation in Construction*, *181*, 106572. https://doi.org/10.1016/j.autcon.2025.106572
11. Martins, M., Lameiras, R., & Alencar, G. (2023). Permanent formwork of textile reinforced concrete (TRC) for composite concrete slabs (Version v1) [Conference paper]. Zenodo. https://doi.org/10.5281/zenodo.8133259
12. Arunothayan, A. R., Ramesh, A., & Sanjayan, J. G. (2024). Fire resistance of 3D printed ultra-high performance concrete panels. *Journal of Building Engineering*, *98*, 111100. https://doi.org/10.1016/j.jobe.2024.111100

1. Buswell, R. A., De Silva, W. L., Jones, S. Z., & Dirrenberger, J. (2018). 3D printing using concrete extrusion: A roadmap for research. *Cement and Concrete Research*, *112*, 37–49. https://doi.org/10.1016/j.cemconres.2018.05.006.
2. Jipa, A., & Dillenburger, B. (2022). 3D printed formwork for concrete: State-of-the-art, opportunities, challenges, and applications. *3D Printing and Additive Manufacturing*, *9*(2), 84–107. https://doi.org/10.1089/3dp.2021.0024.
3. Nan, B., Qiao, Y., Leng, J., & Bai, Y. (2025). Advancing structural reinforcement in 3D-printed concrete: Current methods, challenges, and innovations. *Materials*, *18*(2), 252. https://doi.org/10.3390/ma18020252.
4. Zhu, B., Nematollahi, B., Pan, J., et al. (2021). 3D concrete printing of permanent formwork for concrete column construction. *Cement and Concrete Composites*, *121*, 104039. https://doi.org/10.1016/j.cemconcomp.2021.104039.
5. Jipa, A., Bernhard, M., Meibodi, M., et al. (2016). 3D-printed stay-in-place formwork for topologically optimized concrete slabs. In *TxA Emerging Design + Technology* (pp. 97–107). UCL Press. https://doi.org/10.3929/ethz-b-000237082
6. Bedarf, P., Calvo-Barentin, C., Martinez Schulte, D., Şenol, A., Jeoffroy, E., & Dillenburger, B. (2023). Mineral composites: Stay-in-place formwork for concrete using foam 3D printing. *Architecture, Structures and Construction*, *3*(2), 251–262. https://doi.org/10.1007/s44150-023-00084-x.
7. Guan, J., Wang, L., Huang, Y., & Ma, G. (2025). 3D printed concrete composite slabs fabricated by prestress reinforced permanent formwork: Design, manufacturing, and performance. *Engineering Structures*, *325*, 119446. https://doi.org/10.1016/j.engstruct.2024.119446.
8. Raza, S., Manshadi, B., Sakha, M., Widmann, R., Wang, X., Fan, H., & Shahverdi, M. (2025). Load transfer behavior of 3D printed concrete formwork for ribbed slabs under eccentric axial loads. *Engineering Structures*, *322*, 119148. https://doi.org/10.1016/j.engstruct.2024.119148.
9. Raza, S., Sakha, M., Hassan, Z., Manshadi, B., Wang, X., Fan, H., Dillenburger, B., & Shahverdi, M. (2025). Flexural behavior of stay-in-place load-bearing 3D-printed concrete formwork for ribbed slabs. *Engineering Structures*, *338*, 120531. https://doi.org/10.1016/j.engstruct.2025.120531.
10. Sakha, M., Raza, S., Wang, X., Fan, H., Pichler, N., & Shahverdi, M. (2026). Design optimization and assessment of stay-in-place 3D printed concrete formwork for slabs. *Automation in Construction*, *181*, 106572. https://doi.org/10.1016/j.autcon.2025.106572
11. Martins, M., Lameiras, R., & Alencar, G. (2023). Permanent formwork of textile reinforced concrete (TRC) for composite concrete slabs (Version v1) [Conference paper]. Zenodo. https://doi.org/10.5281/zenodo.8133259
12. Arunothayan, A. R., Ramesh, A., & Sanjayan, J. G. (2024). Fire resistance of 3D printed ultra-high performance concrete panels. *Journal of Building Engineering*, *98*, 111100. https://doi.org/10.1016/j.jobe.2024.111100

13. Reznik, P. A., Petrenko, D. H., Volodymyrov, A. V., Alataiev, D. A., & Maksymenko, V. O. (2025). Strength anisotropy of 3D-printed concrete: Experimental investigation and statistical analysis. *Scientific Bulletin of Construction*, *112*(1), 248–255. https://doi.org/10.33042/2311-7257.2025.112.1.30

14. Guan, J., Wang, L., Huang, Y., Ma, G., & Tao, Y. (2024). Evaluation of the performance of reinforced concrete beams with 3D-printed permanent formwork. *Journal of Intelligent Construction*, *2*(4), 9180030. https://doi.org/10.26599/JIC.2024.9180030

15. Budiman, F., Halim, A., Chandra, J., & Pudjisuryadi, P. (2023). Flexural and shear behavior of 3D printed reinforced concrete beams: An experimental study. *Civil Engineering Dimension*, *25*(1), 1–9. https://ced.petra.ac.id/index.php/civ/article/view/25350

16. Ter Haar, B., Kruger, J., & van Zijl, G. (2024). Off-site 3D printed concrete beam design and fabrication. *Journal of Building Engineering*, *89*, 109117. https://doi.org/10.1016/j.jobe.2024.109117

17. Gebhard, L., Mata-Falcón, J., Anton, A., Dillenburger, B., & Kaufmann, W. (2021). Structural behaviour of 3D printed concrete beams with various reinforcement strategies. *Engineering Structures*, *240*, 112380. https://doi.org/10.1016/j.engstruct.2021.112380

18. Chen, Y., Zhang, W., Zhang, Y., Liu, Z., et al. (2025). A novel in-process rebar integration method for 3D printing reinforced concrete beams and performance evaluation. *Virtual and Physical Prototyping*, *20*(1). https://doi.org/10.1080/17452759.2025.2536556

19. Zhang, S., Kalus, M., Engel, S., Hegger, J., & Claßen, M. (2023). Development of an innovative 3D-printing process for reinforced concrete – AMoRC method. In A. Jędrzejewska et al. (Eds.), *SynerCrete 2023: International RILEM Conference* (RILEM Bookseries, Vol. 44, pp. 641–652). Springer. https://doi.org/10.1007/978-3-031-33187-9_59

20. Qiu, M., Qian, Y., Sun, Y., & Leung, C. K. Y. (2025). Flexural performance of concrete beams via 3D printing stay-in-place formwork followed by casting of normal concrete. *Journal of Sustainable Cement-Based Materials*, *14*(3), 417–430. https://doi.org/10.1080/21650373.2024.2377275

21. Bong, S. H., Nematollahi, B., Mechtcherine, V., Li, V. C., & Khayat, K. (2024). Three-dimensional-printed engineered, strain-hardening geopolymer composite as permanent formwork for construction of reinforced concrete beam. *ACI Structural Journal*, *121*(2), 37–48. https://doi.org/10.14359/51739159

22. Qiu, M., Qian, Y., & Dai, J.-G. (2024). Enhancing the flexural performance of concrete beams with 3D-printed UHP-SHCC permanent formwork via graded fiber volume fraction. *Composite Structures*, *341*, 118211. https://doi.org/10.1016/j.compstruct.2024.118211

23. Wang, C., Yin, S., Zhao, Y., & Li, Y. (2025). Flexural behavior of composite beams with textile reinforced concrete (TRC) permanent formwork considering interface characteristics. *Journal of Building Engineering*, *99*, 111602. https://doi.org/10.1016/j.jobe.2024.111602

24. Wang, H., Shen, J., Sun, X., Dong, W., & Gao, J. (2025). Numerical investigation on shear behaviour of reinforced concrete beam with 3D printed concrete permanent formwork. *Journal of Building Engineering*, *100*(11), 111706. https://doi.org/10.1016/j.jobe.2024.111706

13. Reznik, P. A., Petrenko, D. H., Volodymyrov, A. V., Alataiev, D. A., & Maksymenko, V. O. (2025). Strength anisotropy of 3D-printed concrete: Experimental investigation and statistical analysis. *Scientific Bulletin of Construction*, *112*(1), 248–255. https://doi.org/10.33042/2311-7257.2025.112.1.30

14. Guan, J., Wang, L., Huang, Y., Ma, G., & Tao, Y. (2024). Evaluation of the performance of reinforced concrete beams with 3D-printed permanent formwork. *Journal of Intelligent Construction*, *2*(4), 9180030. https://doi.org/10.26599/JIC.2024.9180030

15. Budiman, F., Halim, A., Chandra, J., & Pudjisuryadi, P. (2023). Flexural and shear behavior of 3D printed reinforced concrete beams: An experimental study. *Civil Engineering Dimension*, *25*(1), 1–9. https://ced.petra.ac.id/index.php/civ/article/view/25350

16. Ter Haar, B., Kruger, J., & van Zijl, G. (2024). Off-site 3D printed concrete beam design and fabrication. *Journal of Building Engineering*, *89*, 109117. https://doi.org/10.1016/j.jobe.2024.109117

17. Gebhard, L., Mata-Falcón, J., Anton, A., Dillenburger, B., & Kaufmann, W. (2021). Structural behaviour of 3D printed concrete beams with various reinforcement strategies. *Engineering Structures*, *240*, 112380. https://doi.org/10.1016/j.engstruct.2021.112380

18. Chen, Y., Zhang, W., Zhang, Y., Liu, Z., et al. (2025). A novel in-process rebar integration method for 3D printing reinforced concrete beams and performance evaluation. *Virtual and Physical Prototyping*, *20*(1). https://doi.org/10.1080/17452759.2025.2536556

19. Zhang, S., Kalus, M., Engel, S., Hegger, J., & Claßen, M. (2023). Development of an innovative 3D-printing process for reinforced concrete – AMoRC method. In A. Jędrzejewska et al. (Eds.), *SynerCrete 2023: International RILEM Conference* (RILEM Bookseries, Vol. 44, pp. 641–652). Springer. https://doi.org/10.1007/978-3-031-33187-9_59

20. Qiu, M., Qian, Y., Sun, Y., & Leung, C. K. Y. (2025). Flexural performance of concrete beams via 3D printing stay-in-place formwork followed by casting of normal concrete. *Journal of Sustainable Cement-Based Materials*, *14*(3), 417–430. https://doi.org/10.1080/21650373.2024.2377275

21. Bong, S. H., Nematollahi, B., Mechtcherine, V., Li, V. C., & Khayat, K. (2024). Three-dimensional-printed engineered, strain-hardening geopolymer composite as permanent formwork for construction of reinforced concrete beam. *ACI Structural Journal*, *121*(2), 37–48. https://doi.org/10.14359/51739159

22. Qiu, M., Qian, Y., & Dai, J.-G. (2024). Enhancing the flexural performance of concrete beams with 3D-printed UHP-SHCC permanent formwork via graded fiber volume fraction. *Composite Structures*, *341*, 118211. https://doi.org/10.1016/j.compstruct.2024.118211

23. Wang, C., Yin, S., Zhao, Y., & Li, Y. (2025). Flexural behavior of composite beams with textile reinforced concrete (TRC) permanent formwork considering interface characteristics. *Journal of Building Engineering*, *99*, 111602. https://doi.org/10.1016/j.jobe.2024.111602

24. Wang, H., Shen, J., Sun, X., Dong, W., & Gao, J. (2025). Numerical investigation on shear behaviour of reinforced concrete beam with 3D printed concrete permanent formwork. *Journal of Building Engineering*, *100*(11), 111706. https://doi.org/10.1016/j.jobe.2024.111706

25. Lee, M., Mata-Falcón, J., & Kaufmann, W. (2022). Shear strength of concrete beams using stay-in-place flexible formworks with integrated transverse textile reinforcement. *Engineering Structures, 271*, 114970. https://doi.org/10.1016/j.engstruct.2022.114970

26. Li, L., Shang, C., & Wang, X. (2025). Study on the shear performance of MMOM stay-in-place formwork beams reinforced with perforated steel pipe skeleton. *Buildings, 15*(15), 2638. https://doi.org/10.3390/buildings15152638

27. Demchyna, B., Vozniuk, L., Surmai, M., Havryliak, S., & Famulyak, Y. (2023). Experimental study of the dome model made using a 3D printer from PLA plastic. *AIP Conference Proceedings, 2949*(1), 020025. https://doi.org/10.1063/5.0165270

28. Demchyna, B., Vozniuk, L., Surmai, M., Burak, D., & Shcherbakov, S. (2024). 3D printing technology for monolithic beams with the possibility of reinforcing bars. *Bulletin of Lviv National Environmental University. Series Architecture and Construction, 25*, 32–37. https://doi.org/10.31734/architecture2024.25.032

29. Reznik, P., Lugchenko, O., Volodymyrov, A., Tenesesku, V., Alatayev, D., & Buldakov, O. (2025). Numerical analysis of 3D printed permanent formwork for reinforced concrete. *Collected Scientific Works of the Ukrainian State University of Railway Transport, 212*, 82–100. https://doi.org/10.18664/1994-7852.212.2025.336411

30. Kalmykov, O., Gaponova, L., Reznik, P., & Grebenchuk, S. (2017). Use of information technologies for energetic portrait construction of cylindrical reinforced concrete shells. *MATEC Web of Conferences, 116*, 02017. https://doi.org/10.1051/matecconf/201711602017

31. Shmukler, V. S., Vozniuk, L. I., & Berezhna, K. V. (2022). Energy portrait of the structural system as a criteria for option design. *Bulletin of Kharkov National Automobile and Highway University, 98*, 136–143. https://doi.org/10.30977/BUL.2219-5548.2022.98.0.136

32. Kalmykov, O. O., Reznik, P. A., V'iunkovskyi, V. P., Demianenko, I. M., & Buldakov, O. O. (2025). Towards the optimization of reinforced concrete slab topology. *Municipal Economy of Cities. Series: Information Technology and Engineering, 192*, 228–235. https://doi.org/10.33042/3083-6727-2025-4-192-228-235

33. Shmukler, V., Petrova, O., Reznik, P., Hamad, F. S., & Sosnowska, M. (2019). Improvement of the structural parameters of the reinforced concrete support in a mesh cage. *AIP Conference Proceedings, 2077*(1), 020048. https://doi.org/10.1063/1.5091909

34. Nguyen, M. H., Phan, H. N., Fujikura, S., Thay, V., Nguyen, V. H., Pham, N. P., & Mai, T. T. T. (2025). Experimental and theoretical analyses for flexural performance of reinforced concrete beams using ultra-high-performance concrete permanent formwork panels embedded with reinforcement grids. *Structural Concrete*, 1–25. https://doi.org/10.1002/suco.70392

35. ДСТУ Б В.2.6-156:2010. Конструкції будинків і споруд. Бетонні та залізобетонні конструкції з важкого бетону. Правила проектування. Національний стандарт України. Чинний від 01.06.2011. Київ: Мінрегіонбуд України, 2011.

25. Lee, M., Mata-Falcón, J., & Kaufmann, W. (2022). Shear strength of concrete beams using stay-in-place flexible formworks with integrated transverse textile reinforcement. *Engineering Structures, 271*, 114970. https://doi.org/10.1016/j.engstruct.2022.114970

26. Li, L., Shang, C., & Wang, X. (2025). Study on the shear performance of MMOM stay-in-place formwork beams reinforced with perforated steel pipe skeleton. *Buildings, 15*(15), 2638. https://doi.org/10.3390/buildings15152638

27. Demchyna, B., Vozniuk, L., Surmai, M., Havryliak, S., & Famulyak, Y. (2023). Experimental study of the dome model made using a 3D printer from PLA plastic. *AIP Conference Proceedings, 2949*(1), 020025. https://doi.org/10.1063/5.0165270

28. Demchyna, B., Vozniuk, L., Surmai, M., Burak, D., & Shcherbakov, S. (2024). 3D printing technology for monolithic beams with the possibility of reinforcing bars. *Bulletin of Lviv National Environmental University. Series Architecture and Construction, 25*, 32–37. https://doi.org/10.31734/architecture2024.25.032

29. Reznik, P., Lugchenko, O., Volodymyrov, A., Tenesesku, V., Alatayev, D., & Buldakov, O. (2025). Numerical analysis of 3D printed permanent formwork for reinforced concrete. *Collected Scientific Works of the Ukrainian State University of Railway Transport, 212*, 82–100. https://doi.org/10.18664/1994-7852.212.2025.336411

30. Kalmykov, O., Gaponova, L., Reznik, P., & Grebenchuk, S. (2017). Use of information technologies for energetic portrait construction of cylindrical reinforced concrete shells. *MATEC Web of Conferences, 116*, 02017. https://doi.org/10.1051/matecconf/201711602017

31. Shmukler, V. S., Vozniuk, L. I., & Berezhna, K. V. (2022). Energy portrait of the structural system as a criteria for option design. *Bulletin of Kharkov National Automobile and Highway University, 98*, 136–143. https://doi.org/10.30977/BUL.2219-5548.2022.98.0.136

32. Kalmykov, O. O., Reznik, P. A., V'iunkovskyi, V. P., Demianenko, I. M., & Buldakov, O. O. (2025). Towards the optimization of reinforced concrete slab topology. *Municipal Economy of Cities. Series: Information Technology and Engineering, 192*, 228–235. https://doi.org/10.33042/3083-6727-2025-4-192-228-235

33. Shmukler, V., Petrova, O., Reznik, P., Hamad, F. S., & Sosnowska, M. (2019). Improvement of the structural parameters of the reinforced concrete support in a mesh cage. *AIP Conference Proceedings, 2077*(1), 020048. https://doi.org/10.1063/1.5091909

34. Nguyen, M. H., Phan, H. N., Fujikura, S., Thay, V., Nguyen, V. H., Pham, N. P., & Mai, T. T. T. (2025). Experimental and theoretical analyses for flexural performance of reinforced concrete beams using ultra-high-performance concrete permanent formwork panels embedded with reinforcement grids. *Structural Concrete*, 1–25. https://doi.org/10.1002/suco.70392

35. Ministry of Regional Development and Construction of Ukraine. (2011). DSTU B V.2.6-156:2010. *Buildings and structures. Heavy concrete and reinforced concrete structures. Design rules* [National standard of Ukraine]. Kyiv, Ukraine.

Резнік П.А. *
Харківський національний університет міського господарства імені О.М. Бекетова
https://orcid.org/0000-0003-3937-6833

Володимиров А.В.
Харківський національний університет міського господарства імені О.М. Бекетова
https://orcid.org/0009-0001-8416-535X

Алатаєв Дж.А.
Харківський національний університет міського господарства імені О.М. Бекетова
https://orcid.org/0000-0003-1570-8469

Максименко В.О.
Харківський національний університет міського господарства імені О.М. Бекетова
https://orcid.org/0009-0007-3771-0857

Експериментально-чисельне дослідження повномасштабних залізобетонних балок із 3D-друкованою незнімною опалубкою

Аннотація. У статті наведено оцінку ефективності коробчастої незнімної опалубки, виготовленої за технологією 3D-друку бетону, для повномасштабних залізобетонних балок шляхом її експериментально-теоретичного аналізу. В роботі встановлено вплив 3D-друкованої оболонки на жорсткість, тріщиностійкість і граничну несучу здатність при чотириточковому згині, а також виконано чисельну верифікацію результатів та оцінку за енергетичним критерієм. Проведено повномасштабне випробування 8 балок однакової геометрії (L=3220 мм, b=200 мм, h=320 мм) із бетонним ядром класу С20/25 та 3D-друкованою оболонкою, матеріальні характеристики якої прийнято за попереднім експериментальним дослідженням і наближено до класу С16/20. Розглянуто зразки з малим поперечним армуванням, без поперечного армування, а також з поперечим армуванням та локальними пошкодженнями оболонки. Візуальні спостереження підтвердили згинно-зсувний механізм руйнування з домінуючою похилою тріщиною в приопорній зоні та відсутність протяжної деламінації оболонки від ядра. Порівняння з нормативними показниками міцності показало близькі розрахункові рівні за згином (MRd 34.2 кНм для RC+3DCP та 32.7 кНм для RC) і суттєву різницю за поперечною силою. Нелінійні моделі з мікроплощинною моделлю бетону відтворили огинаючу експериментальних кривих; гранична сила становила 81.9 кН для варіанта з опалубкою та 77.1 кН без опалубки. Енергетичний аналіз за критерієм Василькова–Шмуклера показав концентрацію щільності потенційної енергії деформації у зонах тріщиноутворення та зменшення сумарної енергії для бетонного ядра з друкованою опалубкою до 49.64% в порівнянні з чисто бетонною конструкцією при однакових зовнішніх діях, що інтерпретується як підвищення жорсткості і ефективніша зсувна робота композитного перерізу. Результати обґрунтовують доцільність застосування 3D-друкованої опалубки та окреслюють кроки до масштабування рішення на повторювані елементи і вузли каркасних систем.

Ключові слова: 3D-друк бетону, незнімна опалубка, залізобетонна балка, метод скінченних елементів, потенційна енергія деформації.

*Адреса для листування E-mail: Petro.Reznik@kname.edu.ua

Надіслано до редакції:	02.12.2025	Прийнято до друку після рецензування:	18.12.2025	Опубліковано (оприлюднено):	26.12.2025

Suggested Citation:

APA style: Reznik, P., Volodymyrov, A., Alataiev, D., & Maksymenko, V. (2025). Experimental and numerical study of full-scale reinforced concrete beams with 3DCP permanent formwork. *Academic Journal Industrial Machine Building Civil Engineering*, *2*(65), 97–108. https://doi.org/10.26906/znp.2025.65.4215

DSTU style: Experimental and numerical study of full-scale reinforced concrete beams with 3DCP permanent formwork / P. Reznik et al. *Academic journal. Industrial Machine Building, Civil Engineering*. 2025. Vol. 65, iss. 2. P. 97–108. URL: https://doi.org/10.26906/znp.2025.65.4215.